

Cooperative Jahn-Teller effect in the garnets

Z. A. Kazeř, P. Novak,¹⁾ and V. I. Soklov

Moscow State University

(Submitted 12 April 1982)

Zh. Eksp. Teor. Fiz. 83, 1483–1499 (October 1982)

The cooperative Jahn-Teller effect (CJTE) is investigated experimentally and theoretically in compounds having the garnet structure, and containing octahedral Mn^{3+} and Cu^{2+} ions with the E_g electronic ground state. Data on the critical temperatures of the phase transitions and the magnitudes of the tetragonal distortions induced by the CJTE are obtained from x-ray investigations and measurements of the elastic, magnetic, and magnetostriction properties in the temperature range 4.2–600 K. The critical concentrations of the Jahn-Teller ions and the temperature dependences of the order parameters are determined, and the unusual metamagnetic transition that occurs in the manganese garnet below the antiferromagnetic transition temperature is studied. It is shown that the characteristics of the CJTE in the garnets can be described within the framework of a simple model with nonferroelastic ordering of the local Jahn-Teller distortions. Equilibrium configurations that allow the experimental data on the temperature and concentration dependences of the CJTE in the garnets to be explained qualitatively are found on the basis of the assumptions of the model. The magnetic properties and the behavior of garnets with Jahn-Teller-ion concentrations lower than the critical concentration are discussed.

PACS numbers: 71.70.Ej, 75.80. + q, 75.30.Kz

1. INTRODUCTION

Materials containing ions with orbitally degenerate ground states—the so-called Jahn-Teller (JT) ions—exhibit a number of qualitative anomalies in their physical properties. This is due to the instability of the ligand configuration around such ions against distortions that lower symmetry of the configuration. Compounds with JT ions have been the subject of quite a large number of investigations, for which there are good reviews.^{1–4} In concentrated systems, i.e., in systems in which the number of JT ions is fairly high, the lowering of the symmetry of the environment of the ion has a correlated cooperative character. This phenomenon, which causes the lowering of the symmetry of the whole crystal by inducing a phase transition at some temperature T_{JT} , is usually called the cooperative Jahn-Teller effect (CJTE). At present the CJTE and its influence on the various physical properties of solids have been quite thoroughly studied for materials with the perovskite, spinel, rutile, and zircon structures.^{3–6}

In the present paper we present experimental data on, and consider a theoretical model for, the characteristics of the CJTE in compounds with the garnet structure. We have already reported the experimental observation of the CJTE in garnets with octahedral Mn^{3+} and Cu^{2+} ions and a theoretical approach to the description of their properties in brief communications.^{7,8}

Since Mn^{3+} and Cu^{2+} are JT ions in the spinel structure as well, let us first of all note some important—in our opinion—characteristics of the CJTE in the garnets and spinels. Spinels with octahedral Mn^{3+} and Cu^{2+} ions always exhibit a tetragonal unit-cell distortion with $(c/a - 1) > 0$. In the garnets both tetragonal elongation of the unit cell

(Mn^{3+}) and tetragonal contraction (Cu^{2+}) are observed. At the same time, the value of $|(c/a - 1)|$ for the garnets is significantly smaller than the value for the spinels (when allowance is made for the relative number of JT ions). In the spinels, the higher T_{JT} is, the greater is the value of $|(c/a - 1)|$ at $T = 0$ K. In the garnets, the opposite situation is possible: the value of $|(c/a - 1)|$ for the copper garnet is five times greater than the corresponding value in the manganese garnet, whereas the T_{JT} of the latter is two times higher than the T_{JT} in a garnet with Cu^{2+} .

Below we shall show that these characteristics can be explained if we assume that the ordering of the local JT distortions in the garnets has a nonferroelastic character. Also, in order to carry out a comparison with the corresponding experimental data, we shall analyze within the framework of the proposed model the temperature dependence of the tetragonal lattice distortion and the rapid disappearance of the CJTE as the JT ions in the garnets are replaced.

Earlier it was established^{9,10} that a garnet containing Mn^{3+} at the octahedral sites exhibits antiferromagnetic order at $T_N = 13.85$ K. The complicated noncollinear magnetic structure deduced for the manganese garnet below T_N from neutron-diffraction data by Plumier *et al.*^{11,12} makes for the unusual metamagnetic transition reported in Refs. 13 and 14. According to measurements,⁹ the antiferromagnetic ordering does not occur in a garnet with Cu^{2+} ions at the octahedral sites right down to 1.6 K.²⁾

To obtain information about the influence of the CJTE on the magnetic properties of the garnets, we measured the magnetic susceptibility, the magnetization, and the magnetostriction of garnets with Mn^{3+} and Cu^{2+} JT ions in the liquid-helium-temperature region. But the mechanism un-

derlying the interrelationship between the magnetic characteristics and the specific structure of the JT lattice distortions deserves, in our opinion, a separate investigation.

2. THE EXPERIMENTAL PART

2.1. Samples and measurement procedure

In the present work we investigated single-crystal samples of the garnet $\text{Ca}_3[\text{Mn}_2^{3+}]\text{Ge}_3\text{O}_{12}$ (MnGeG) and polycrystalline samples of $\text{NaCa}_2[\text{Cu}_2^{2+}]\text{V}_3\text{O}_{12}$ (CuVG), $\text{Ca}_3[\text{Mn}_x\text{Ga}_{2-x}]\text{Ge}_3\text{O}_{12}$ with $0 < x < 2$ (MnGaGeG), and $\text{NaCa}_2[\text{Cu}_x\text{Zn}_{2-x}]\text{V}_3\text{O}_{12}$ with $1 < x < 2$ (CuZnVG). The crystals were grown by B. V. Mill' by the solution-in-the-melt method, and the polycrystalline samples were prepared, using the ceramic technology with two-stage firing in air at temperatures $\sim 1250^\circ\text{C}$ (MnGaGeG) and 640°C (CuZnVG). X-ray phase analysis showed that all the samples, with the exception of the CuVG sample, are single-phase to within $\sim 1\%$. A weak ($\sim 2\%$) admixed CuO line was observed in CuVG.

The magnetic susceptibility and the magnetization were measured in the temperature range 2.0–70 K in fields of up to 60 kOe with a vibrating magnetometer.¹⁵ The sensitivity of the setup is $1.5 \times 10^{-3} \text{ G}\cdot\text{cm}^3$, and the relative measurement error is 1.5%. The longitudinal magnetostriction was measured with a capacitance transducer connected in the tuned circuit of a highly stable cryogenic oscillator operating at a frequency of 1.5 MHz.¹⁶ The smallest magnetostrictive distortion that could be measured was 10 Å, and the relative measurement error was $\sim 5\%$. The temperature and magnetic-field ranges were 2.0–70 K and 0.5–50 kOe respectively. The temperature in both setups was measured with Allen-Bradley carbon resistance thermometers (1/8 W, $R_{300\text{K}} = 270\Omega$), and was stabilized to within $\pm 0.05 \text{ K}$ by a DTS-2 temperature regulator.

The elastic properties of the garnets (Young's modulus and internal friction) were measured by the composite-resonator method on a set-up similar to the one described in Ref. 17. The operating frequency was $\sim 160 \text{ kHz}$, and the measurements were performed in the temperature range 4.2–600 K.

The x-ray investigations were performed on a "Geigerflex" diffractometer (Cu $K\alpha$ and Cu $K\beta$ emission) whose flow-through helium cryostat and high-temperature attachment allow us to realize the 4.2–600-K temperature range.

2.2. The x-ray investigations

Figures 1 and 2 show the temperature dependences of the unit-cell parameters (a , c) and the magnitude of the distortion ($c/a - 1$) of MnGeG and CuVG. The reflection splitting observed at low temperatures indicates the tetragonal distortion of the crystal lattice, and the values of the distortions at 4.2 K were $(c/a - 1) = 3 \times 10^{-3}$ for MnGeG and $(c/a - 1) = -15 \times 10^{-3}$ in CuVG. It can be seen from Figs. 1 and 2 that the $|(c/a - 1)|$ values decrease monotonically with increasing temperature, vanishing at $T_{\text{JT}} = 525 \text{ K}$ (MnGeG) and $T_{\text{JT}} = 250 \text{ K}$ (CuVG).

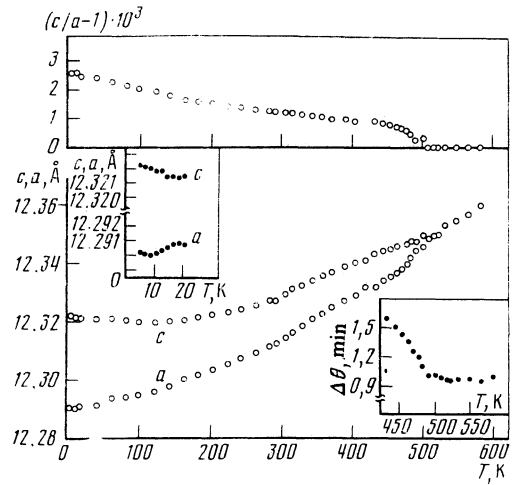


FIG. 1. Temperature dependences of the lattice constants a and c , the halfwidth $\Delta\theta$ of the diffraction peak, and the degree of tetragonal distortion $(c/a - 1)$ of the garnet MnGeG.

The measurements in the case of MnGeG were performed on a single-crystal (100)-cut plate, using the (16.00) ($2\theta \approx 130^\circ$) reflection in Cu $K\beta$ radiation. Below T_{JT} , we observe JT "domains," i.e., regions with different orientations of the tetragonal axis c , in the crystal. Choosing for the investigations those MnGeG samples in which the intensities of the diffraction lines from the domains with c axes parallel and perpendicular to the (100) plane (the plane of cut) were approximately equal, we determined the $(c/a - 1)$ for MnGeG from the halfwidth $\Delta\theta$ of the diffraction peak at $T \approx T_{\text{JT}}$, where a clear resolution of the lines is not observed. The dependence $\Delta\theta(T)$ is shown in the lower inset of Fig. 1. The upper inset in this figure illustrates on an enlarged scale the appearance of additional deformation of the MnGeG unit cell in the region of the antiferromagnetic transition temperature. The symmetry of the crystal does not change in the process: $\Delta c/c = -\Delta a/a = (5.7 \pm 0.8) \times 10^{-5}$ and the change in volume is equal to $\Delta V/V = (\Delta c + 2\Delta a)/c = -(5.7 \pm 2.0) \times 10^{-5}$.

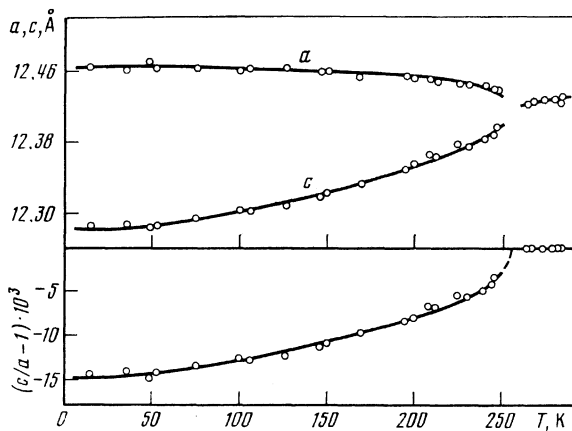


FIG. 2. Temperature dependences of the lattice constants a and c and the degree of tetragonal distortion $(c/a - 1)$ of the garnet CuVG.

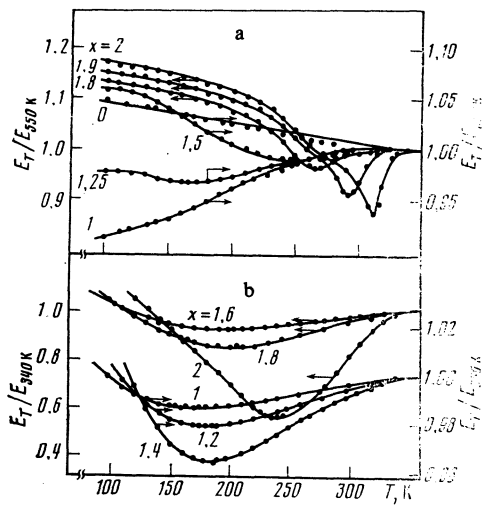


FIG. 3. Temperature dependence of the relative Young moduli for: a) MnGaGeG and b) CuZnVG. In Fig. a the temperature scale is 100 K.

The parameters of the CuVG lattice were measured on polycrystalline samples, using the (880) and (088 + 808) ($2\theta \approx 89^\circ$) reflections in Cu K_α radiation. The error in the determination of a and c was $\sim 10^{-3} \text{ \AA}$, which is an order of magnitude worse than the error in the MnGeG case.

2.3. Young's modulus (E) and internal friction (Q^{-1})

Figure 3 shows the temperature dependences of the relative magnitudes of Young's moduli for MnGaGeG and CuZnVG. It can be seen that the sharp E anomalies observed in the MnGeG and CuVG samples correspond to the temperature T_{JT} determined by the x-ray method. As the JT ions are replaced by Ga^{3+} or Zn^{2+} , these anomalies decrease significantly in magnitude, get smeared, and shift toward the region of lower temperatures. The values of E for MnGaGeG with $0.5 < x < 1.0$ are found to decrease monotonically in the temperature range 500–40 K, while the values for samples with $x < 0.5$ are found to increase slightly with decreasing temperature.

In the region $T < 40 \text{ K}$, the Young moduli of the investigated garnets increase rapidly with decreasing temperature. This is illustrated by Fig. 4, in which, as an example, we

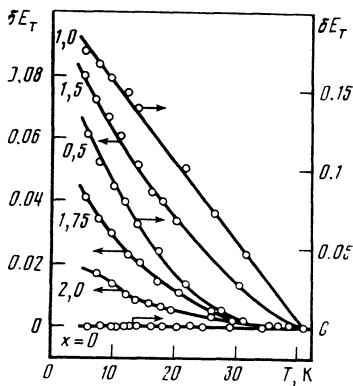


FIG. 4. Variation of the relative Young moduli $\delta E_T = (E_T/E_{40K} - 1)$ of the system MnGaGeG in the low-temperature region.

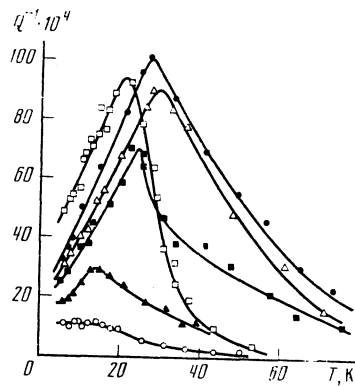


FIG. 5. Behavior of the internal friction of the system MnGaGeG at low temperatures: \circ) $x = 2.0$; \blacktriangle) 1.75; \blacksquare) 1.50; \triangle) 1.25; \bullet) 1.0; \square) 0.5.

depict the variation with temperature of the relative Young modulus $\delta E_T = (E_T/E_{40K} - 1)$ for the system MnGaGeG. Notice that δE_T varies nonmonotonically with varying JT-ion concentration: it attains a maximum at $x = 0.75$, and subsequently decreases with increasing x (i.e., with increasing Mn^{3+} concentration). The increase of δE_T is accompanied by the appearance of internal-friction anomalies (Fig. 5): the dependences $Q^{-1}(T)$ possess in the vicinity of $T_{max} \approx 30 \text{ K}$ peaks that attain their greatest height in the garnets with $0.75 \leq x \leq 1.25$, and practically do not shift along the temperature axis as x is varied.

The elastic properties of CuZnVG are found to behave in a similar manner at low temperatures: the quantity $\delta E_{4.2K}$ (for $x = 1.0$) is also ~ 0.20 and the value of $T_{max} \approx 40 \text{ K}$.

2.4. The magnetic susceptibility and the magnetization (MnGaGeG)

In Table I we present the lattice constants and the principal magnetic characteristics of MnGaGeG, obtained from measurements of the temperature dependence of the magnetic susceptibility. The $\chi(T)$ curves for samples with $x \geq 1$ exhibit peaks in the liquid-helium-temperature region, which indicate the appearance of long-range magnetic order. The Néel temperature (T_N) decreases linearly with decreasing Mn^{3+} content. The extrapolation of $T_N(x)$ allows us to find the value of the critical magnetic-ion concentration, i.e., the concentration at which long-range magnetic order does not occur even at $T = 0 \text{ K}$: $C_{cr} = x_{cr}/2 = 0.31 \pm 0.02$. This value coincides within the limits of the experimental error with the theoretical C_{cr} value¹⁸ predicted by percolation theory for the eight closest neighbors of the octahedral sublattice of a garnet.

In the paramagnetic region χ varies with temperature according to the Curie-Weiss law with the paramagnetic Curie temperatures Θ_p given in Table I. The calculation of the effective magnetic moments (P_{eff}) of the investigated MnGaGeG samples shows that, as x increases, the deviation of P_{eff} from the theoretical value, $P_{eff}^{theor} = g[s(s+1)]^{1/2} = 4.9\mu_B$, for the free Mn^{3+} ion increases.

Below the antiferromagnetic transition temperature, the magnetization isotherms of a MnGeG single crystal exhibit jumps, which, according to Ref. 13, are due to an un-

TABLE I. The lattice constants and magnetic characteristics of the garnets $\text{Ca}_3\text{Mn}_x\text{Ga}_{2-x}\text{Ge}_3\text{O}_{12}$.

x	$a_0, \text{\AA}$	T_N, K	$-\theta_p, \text{K}$	$P_{\text{eff}}, \mu\text{B}$
2	12.307	13.8	14.3	5.37
1.75	12.298	11.0	12.3	5.27
1.5	12.292	9.0	10.0	5.10
1.25	12.284	6.1	8.5	5.06
1.0	12.277	4.0	7.2	5.00
0.75	12.269	<2	5.0	5.08
0.5	12.261	—	3.0	4.99

sual metamagnetic transition occurring in MnGeG below T_N and the splitting up of the crystal into JT domains at $T < T_{JT}$. In the region $T > T_N$, the $M(H)$ isotherms have the usual—for paramagnetic materials—linear character.

The polycrystalline MnGaGeG samples with $x \geq 1.0$ also exhibit below T_N magnetization jumps that are more smeared than the jumps exhibited by the single-crystal samples: the sharp increases in M occur over magnetic-field ranges of 15–35 kOe.

2.5. Magnetostriction

The results obtained in the measurement of the magnetostriction $\Delta l/l$ of single-crystal and polycrystalline MnGaGeG samples are given in Figs. 6 and 7. The $H-\Delta l/l$ isotherms of the MnGeG crystal at 4.2 K exhibit abrupt jumps at field-intensity values H_{cr} that correspond to the magnetization jumps. Since the crystal contains three types of JT domains differing in the directions of the axes of the tetragonal distortions, there are, in the general case, three jumps in the magnetostriction isotherms. One $\Delta l/l$ jump is observed along the $\langle 111 \rangle$ axis, since in all the three types of domains the c axes make the same angle with \mathbf{H} . As can be seen from Fig. 7, as we raise the temperature or decrease the JT-ion content in the garnet, the anomaly in the $H-\Delta l/l$ curves shifts toward the region of weak fields, and manifests itself much more weakly than the corresponding anomaly for MnGeG. But the magnetostriction data for the MnGaGeG polycrystals indicate that the phase transition continues to occur in a magnetic field right up to the concen-

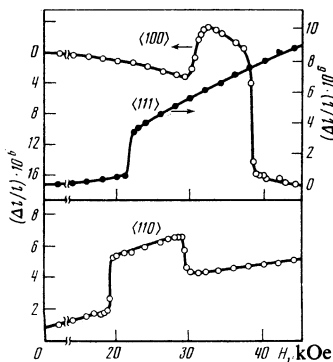


FIG. 6. Magnetostriction isotherms of the MnGeG crystal at 4.2 K in the cases when the magnetic field is oriented along the axes $\langle 100 \rangle$, $\langle 111 \rangle$, and $\langle 110 \rangle$.

tration $x = 1.0$. The $H-\Delta l/l$ isotherms of the paramagnetic samples ($x < 1$) do not follow the H^2 law, which is characteristic of many paramagnetic materials.¹⁹ This is illustrated in Fig. 7, in which, we give as an example magnetostriction isotherms of the garnet with $x = 0.5$.

The magnetostriction of CuZnVG at liquid-helium temperatures is roughly 20 times smaller, and has a paramagnetic character for all compositions.

3. THEORETICAL ANALYSIS

3.1. The model

The electronic ground state of Mn^{3+} and Cu^{2+} in an undistorted octahedron is the orbital doublet E_g . We shall, limiting ourselves to the consideration of the static Jahn-Teller effect (JTE), assume that the electronic doublet interacts only with the pair of normal coordinates Q_e and Q_g of the octahedron, that transform according to the E_g representation of the symmetry group O_h . It should be noted that in the garnet structure the octahedrons surrounding the JT ions are trigonally distorted, and that the individual octahedrons are rotated through an angle of $\sim 28^\circ$ about the $\langle 111 \rangle$ directions. This is analyzed in the Appendix.

Without allowance for the anharmonic terms, the Hamiltonian for an isolated JT center has the form

$$\mathcal{H} = \frac{1}{2}C(Q_e^2 + Q_g^2) - g(Q_e \hat{T}_e + Q_g \hat{T}_g), \quad (1)$$

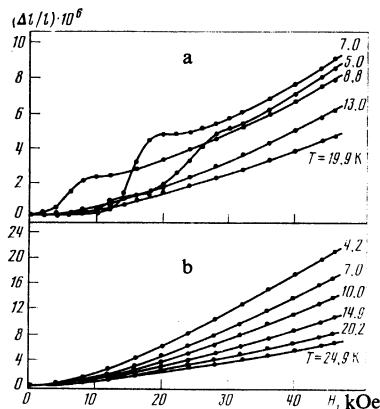


FIG. 7. Magnetostriction isotherms of MnGaGeG with: a) $x = 1.75$ and b) $x = 0.5$.

where \hat{T}_e and \hat{T}_g are the electronic operators of the E_g symmetry, C is the elastic constant, and g is the linear-vibronic-coupling constant. The introduction of the polar coordinates Q and φ ($Q_\varepsilon = Q \sin \varphi$, $Q_\vartheta = Q \cos \varphi$) reduces the problem of determining the ground state of a system containing many JT centers to the problem of finding the angle φ for each center. At 0 K these angles are given by the minimum of energy

$$E = E_A + E_\pi + E_D. \quad (2)$$

Here E_A characterizes the anisotropy of the adiabatic potential of the individual centers, that arises in (1) when allowance is made for the nonlinear vibronic interaction or the anharmonicity of the lattice. Since for a fixed Q the anisotropic term has the form $(-K \cos 3\varphi)$, the most advantageous configuration corresponds to $\varphi = l\pi/3$, where l is even or odd according as the anisotropy parameter K is positive or negative. Notice that $l = 0, 2$, and 4 correspond to tetragonal extensions of the octahedron along the x , y , and z axes, while $l = 3, 5$, and 1 correspond to tetragonal contractions along the same axes. Since a hexagonal extension is always observed for octahedral Mn^{3+} and Cu^{2+} ions in oxides,⁷ we can assume that $K > 0$.

The second term in (2) describes the pair interaction of JT centers in an infinite crystal (i.e., without allowance for the macroscopic distortion), and has, according to Ref. 21, the form

$$E_\pi = \sum_{i=1}^N \sum_{j=1}^N (J_{e_\varepsilon}^{ij} \sin \varphi_i \sin \varphi_j + J_{\vartheta\varepsilon}^{ij} \cos \varphi_i \cos \varphi_j + J_{e_\vartheta}^{ij} \sin \varphi_i \cos \varphi_j + J_{\vartheta\varepsilon}^{ij} \cos \varphi_i \sin \varphi_j). \quad (3)$$

Here the $J_{\alpha\beta}^{ij}$ are interaction constants, the analysis and physical meaning of which will be given in the next subsection, and the summation is over all the N JT centers.

The energy E_D takes account of the interaction of the JT centers with the CJTE-induced macroscopic deformations. If we denote the components of the crystal strain of symmetry E_g by e_ϑ and e_ε , then

$$E_D = \sum_{i=1}^N a_i (e_\vartheta \cos \varphi_i + e_\varepsilon \sin \varphi_i). \quad (4)$$

For a system with one kind of JT ions, the interaction constants do not depend on i , and e_ϑ and e_ε should be proportional to the mean values of Q_ϑ and Q_ε . The expression (4) then assumes the form

$$E_D = a \sum_{i=1}^N (\cos \varphi_i \overline{\cos \varphi} + \sin \varphi_i \overline{\sin \varphi}), \quad (5)$$

where

$$\overline{\cos \varphi} = \frac{1}{N} \sum_{i=1}^N \cos \varphi_i, \quad \overline{\sin \varphi} = \frac{1}{N} \sum_{i=1}^N \sin \varphi_i. \quad (A)$$

Since a macroscopic distortion of the lattice lowers the energy of the JT centers, it is clear that $a < 0$.

3.2. Interaction of the JT centers

To compute the parameters $J_{\alpha\beta}^{ij}$, we must determine the distortion caused by an isolated JT center. Let us, following Ref. 21, introduce the vector $[X_\alpha^a(\mathbf{r}), Y_\alpha^a(\mathbf{r}), Z_\alpha^a(\mathbf{r})]$ ($\alpha = \varepsilon, \vartheta$) characterizing the displacement of the point \mathbf{r} , caused by the JT center a whose configuration is given by the angle $\varphi_a = \pi/2(Q_\vartheta^a = 0, Q_\varepsilon^a \neq 0, \alpha = \varepsilon)$ and $\varphi_a = 0(Q_\vartheta^a \neq 0, Q_\varepsilon^a = 0, \alpha = \vartheta)$. Using the analytic forms of the expressions giving the normal coordinates Q_ε and Q_ϑ as functions of the coordinates X_K, Y_K , and Z_K of the anions, we can easily determine the changes that occur in the normal coordinates Q_ε and Q_ϑ of the center b as a result of the distortion caused by the center a . If we denote these changes by $Q_{\alpha\beta}^{ab}(\alpha = \varepsilon, \vartheta; \beta = \varepsilon, \vartheta)$, then

$$Q_{\varepsilon\varepsilon}^{ab} = 1/2 [X_\varepsilon^a(x_b+r_0, y_b, z_b) - X_\varepsilon^a(x_b-r_0, y_b, z_b) - Y_\varepsilon^a(x_b, y_b+r_0, z_b) + Y_\varepsilon^a(x_b, y_b-r_0, z_b)],$$

$$Q_{\vartheta\vartheta}^{ab} = \frac{1}{2\sqrt{3}} [-X_\vartheta^a(x_b+r_0, y_b, z_b) - X_\vartheta^a(x_b-r_0, y_b, z_b) - Y_\vartheta^a(x_b, y_b+r_0, z_b) - Y_\vartheta^a(x_b, y_b-r_0, z_b) + 2Z_\vartheta^a(x_b, y_b, z_b+r_0) - 2Z_\vartheta^a(x_b, y_b, z_b-r_0)]. \quad (6)$$

Here r_0 is the metal-ligand spacing in the undistorted octahedron and x_b, y_b , and z_b are the coordinates of the center b relative to the center a . Similarly, we can determine $Q_{\varepsilon\vartheta}^{ab}$ and $Q_{\vartheta\varepsilon}^{ab}$.

According to (21), the interaction constants are connected with the $Q_{\alpha\beta}^{ab}$ by the relation

$$J_{\alpha\beta}^{ab} = -g(Q_{\alpha\beta}^{ab} + Q_{\alpha\beta}^{ba})/4; \quad \alpha = \varepsilon, \vartheta, \quad \beta = \varepsilon, \vartheta. \quad (7)$$

The interaction constants $J_{\alpha\beta}^{ab}$ have, on the basis of this formula, a simple physical meaning: they characterize the change that occurs in the energy of the JT center b as a result of the change produced in the Q_α^b of this center by the strain Q_β^a at the center a .

Let us omit here the details of the calculation, based on the theory of elasticity (the analysis is performed under the assumption that the medium is elastically isotropic), of the specific form of the $J_{\alpha\beta}^{ab}$ for the garnets in question, and give only the final result in the form of plots [Fig. 8(a)] of the relative magnitudes of the constants $J_{\alpha\beta}^{ab}$ for the nearest $J_{\alpha\beta}(111)$ and next-nearest $J_{\alpha\beta}(002)$ neighbors against the ratio $\kappa = \lambda/\mu$. Here λ and μ are the Lamé coefficients, whose values for the garnets lie respectively in the intervals $(1-1.25) \times 10^{12}$ and $(0.74-1.15) \times 10^{12}$ dyn/cm². We show the results obtained in the calculation for MnGeG; those obtained in the case of CuVG are not very different. Figure 8(b) illustrates the dependence of the $J_{\alpha\beta}^{ij}$ on the distance between the JT centers for a fixed value of κ without allowance for the trigonal distortions and the fact that the axes of the octahedrons are not parallel.

Let us note that the indicated method of computing the interaction constants on the basis of the theory of elasticity cannot be used when the JT-center spacing is small, but in a number of particular cases the formula (7) allows us to predict the sign and the relative magnitudes of the constants $J_{\alpha\beta}^{ab}$ without carrying out any calculations, it being only suf-

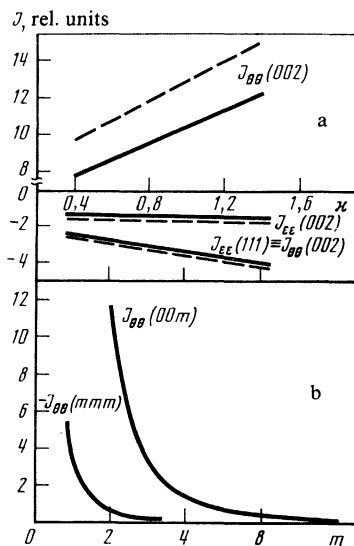


FIG. 8. Dependence of the interaction constants $J_{\alpha\beta}$ ($l mn$) for MnGeG on: a) the parameter κ ; b) the distance between the JT centers for $\kappa = 0.8$. One of the JT centers is located at the coordinate origin; the other, at the point $\frac{1}{2}a_0$ ($l mn$), where a_0 is the lattice constant. The dashed lines correspond to the computations in which allowance was made for the trigonal distortions and the nonparallelism of the axes of the octahedrons.

efficient to take into consideration the fact that the distortion decreases with distance and the displacement is greatest in the force direction. For example, we can show that, for the interaction in a bcc lattice of the next-nearest neighbors located along the cube edge (configuration A), $Q_{\varphi\varphi}^A < 0$ and large, while $Q_{\varepsilon\varepsilon}^A > 0$ and small. Consequently,

$$J_{\varphi\varphi}^A > 0, \quad J_{\varepsilon\varepsilon}^A < 0, \quad |J_{\varphi\varphi}^A| \gg |J_{\varepsilon\varepsilon}^A|. \quad (8)$$

Unfortunately, it is difficult to draw unambiguous conclusions in the case of the interaction of the two nearest neighbors located along the body diagonal of the cube in a bcc lattice (configuration B).

The consideration of the symmetry yields useful relations for the $J_{\alpha\beta}^{ij}$. If we neglect the trigonal distortion of the octahedrons (see, however, the Appendix), then we have for the configurations A and B the relations

$$J_{\varepsilon\varepsilon}^A = J_{\varphi\varphi}^A = J_{\varepsilon\varepsilon}^B = J_{\varphi\varphi}^B = 0 \quad \text{and} \quad J_{\varepsilon\varepsilon}^B = J_{\varphi\varphi}^B. \quad (9)$$

To prove this, it is sufficient to use the transformation of the coordinates Q_ε and Q_φ , and substitute them into (3).

Let us emphasize that, if $J_{\varepsilon\varepsilon}^{ab}$ and $J_{\varphi\varphi}^{ab}$ are negative, then the interaction of the JT centers is ferroelastic, i.e., the configurations for which $\varphi_a = \varphi_b$ are advantageous. Positive $J_{\varepsilon\varepsilon}^{ab}$ and $J_{\varphi\varphi}^{ab}$ make the configurations with $\varphi_b = \varphi_a + \pi$ more advantageous, i.e., correspond to antiferroelastic interaction.

3.3. The equilibrium configurations

The octahedral sites occupied in the garnets in question by the JT ions form a bcc lattice. The division into sublattices should be such that there are no strong antiferroelastic interactions between the centers of the same sublattice. This

means that the centers in the configuration A should not belong to the same sublattice ($J_{\varphi\varphi}^A > 0$). We should impose the same restriction on the centers of the configuration B , since the sign of $J_{\varphi\varphi}^B = J_{\varepsilon\varepsilon}^B$ is not fixed. On the basis of these conditions, it is simplest to divide the lattice into four sublattices in the same way an antiferromagnet with the bcc lattice is divided into magnetic sublattices (when only the interactions of the nearest and the next-nearest neighbors are taken into consideration).

The problem of finding the equilibrium configurations reduces now to the problem of determining the angles φ_i ($i = 1, \dots, 4$) from the equations

$$\partial E / \partial \varphi_i = 0 \quad (i=1, 2, 3, 4). \quad (10)$$

Limiting ourselves to the consideration of the interaction of the nearest and next-nearest neighbors, and taking the formulas (3), (5), and (9) into account, we can write the energy (2) in the form

$$E = \frac{1}{4} N \left\{ J_0 [\cos(\varphi_1 - \varphi_4) + \cos(\varphi_2 - \varphi_3)] + J_1 [\cos(\varphi_1 - \varphi_2) + \cos(\varphi_1 - \varphi_3) + \cos(\varphi_2 - \varphi_4) + \cos(\varphi_3 - \varphi_4)] - K \sum_{i=1}^4 \cos 3\varphi_i + \frac{1}{4} a \sum_{i=1}^4 \sum_{j=1}^4 (\cos \varphi_i \overline{\cos \varphi_j} + \sin \varphi_i \overline{\sin \varphi_j}) \right\}, \quad (11)$$

where we have introduced the notation: $J_0 = 3(J_{\varepsilon\varepsilon}^A + J_{\varphi\varphi}^A)$ and $J_1 = 4J_{\varepsilon\varepsilon}^B$. It follows from the analyses performed in Subsecs. 3.1 and 3.2 that $K > 0$, $a < 0$, and $J_0 > 0$. Furthermore, at 0 K, $\overline{\cos \varphi_i} = \cos \varphi_i^0$ and $\overline{\sin \varphi_i} = \sin \varphi_i^0$, where the φ_i^0 are the equilibrium values of the angles φ_i .

It can be shown that, in the case of strong anisotropy, i.e., for

$$K \gg |J_0 + a/2|, \quad |J_1 + a/2|, \quad (12)$$

the Eqs. (10) possess 5 solutions. The configurations that can be obtained from each other by interchanging the sublattices or the coordinate axes are considered to be identical.

We obtained the solutions for the case in which the relation (12) is not satisfied by the method of successive approximations. The characteristics of the corresponding configurations are given in Table II, and the regions of their stability are shown in Fig. 9. It is natural, when the inequalities (8) are taken into consideration, to assume that the configurations A_1 and A_2 are realized in the garnets in question. Figure 10 schematically shows these configurations for the case of strong anisotropy.

Notice that the configuration A_1 is completely determined by one angle σ_1 , whereas two angles σ_2 and σ_2' are required for the determination of A_2 . In this case, although the macroscopic distortion of the unit cell is always tetragonal, the local distortions of the octahedrons are orthorhombic (with the exception of the case of very strong anisotropy). The angles σ_1 , σ_2 , and σ_2' are functions of the

TABLE II. Principal characteristics of the equilibrium configurations determined by the CJTE in the garnet structure. $|c/a - 1|_{max}$ is the maximum value of the order parameter for a given configuration with reference to the ferroelastically ordered system (F).

Configuration	φ_1	φ_2	φ_3	φ_4	c/a	$ c/a - 1 _{max}$
F	0	0	0	0	$c/a > 1$	1
A_1	$-2\pi/3 - \sigma_1$	$-2\pi/3 - \sigma_1$	$2\pi/3 + \sigma_1$	$2\pi/3 + \sigma_1$	$c/a < 1$	$1/2$
A_2	$-\sigma_2$	$+\sigma_2$	$-2\pi/3 - \sigma_2'$	$2\pi/3 + \sigma_2'$	$c/a > 1$	$1/4$
A_3	$-\sigma_3$	$2\pi/3 + \sigma_3'$	$-2\pi/3 - \sigma_3'$	σ_3	$c/a > 1$	$1/4$
A_4	$-2\pi/3 - \sigma_4$	$2\pi/3 + \sigma_4'$	$2\pi/3 - \sigma_4'$	$-2\pi/3 + \sigma_4$	$c/a < 1$	$1/2$

parameters entering into the energy, and we can compute with their aid the relative value of the macroscopic strain, which, according to (5), is proportional to $\sum_i \cos \varphi_i$. In the case of the configuration A_1 the strain depends only on the quantity $(J_0 + J_1 + a)/K$; in the case of A_2 , on $(J_0 + a/2)/K$ and $(J_1 + a/2)/K$. In Fig. 11 we present the results of numerical calculations of the relative strains for the configurations A_1 and A_2 as functions of the corresponding interaction constants.

4. DISCUSSION OF THE RESULTS

4.1. Concentration dependence of the CJTE in the garnets

The experimental data shown in Fig. 3 indicate that the JTE arises at the appropriate temperatures in samples of MnGaGeG with $x \geq 1.25$ and CuZnVG with $x \geq 1.0$. But the x-ray investigations of the system CuZnVG showed that a sample with $x = 1.8$ remains cubic right down to 4.2 K. The x-ray diffraction pattern for this garnet at 4.2 K did not show even a broadening of the reflections, which would have indicated at least a small distortion of the crystal lattice (the resolving power of the diffractometer in these investigations was 5×10^{-4}). Because of the small magnitude of the tetragonal distortion in MnGeG, we did not carry out an x-ray investigation of the CJTE in MnGaGeG.

The above-noted characteristics give grounds for believing that the JTE in CuZnVG and MnGaGeG with $x \leq 1.8$ does not have a cooperative character, and that the anomalies in the temperature dependences of the Young moduli of the samples with JT-ion concentrations lower than the indicated concentration (Fig. 3) are due to the appearance of correlated distortions of the octahedrons within the boundaries of small regions, i.e. the appearance of JT clusters. Thus, the CJTE in the garnets is characterized by a high critical concentration: ~ 0.9 . Let us, for comparison, note that the critical concentration of the JT ions Mn^{3+} in the spinel $Mn_xCr_{3-x}O_4$ is 0.35 (Ref. 22).

Qualitatively, the mechanism underlying the rapid concentration destruction of the CJTE in the garnets can be understood from the viewpoint of the model ideas developed in Subsecs. 3.1–3.3. Indeed, the introduction of one impurity (i.e., non-Jahn-Teller) center into a ferroelastic JT system will result in the decrease of the order parameter (macroscopic deformation) by an amount proportional to the contribution of the missing JT center. But the ferro-character of the interactions in such a system does not admit of any

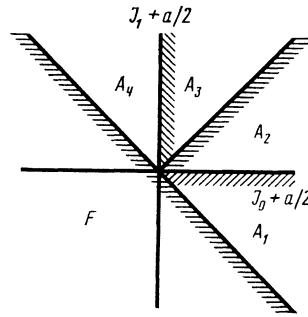


FIG. 9. Stability regions for the phases F and A_1 – A_4 .

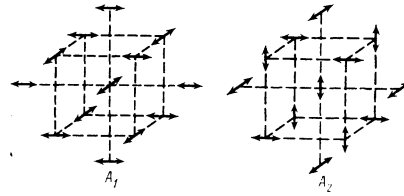


FIG. 10. Diagrammatic representation of the configurations A_1 and A_2 for the case of strong anisotropy. The arrows indicate the tetragonal axes of the extended octahedrons.

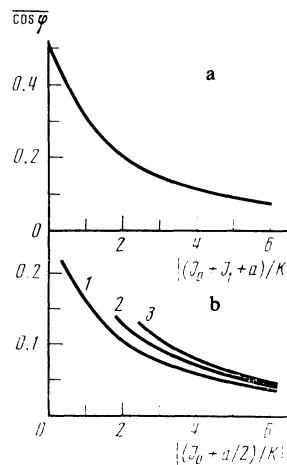


FIG. 11. Dependence of the macroscopic strain on the ratio of the pair-interaction constants to the anisotropy parameter for the configurations: a) A_1 ; b) A_2 . The curves 1, 2, and 3 correspond respectively to the parameter values $|(J_1 + a/2)/K| = 0.3; 1.8, \text{ and } 2.4$.

further reconstruction. On the other hand, substitution in a system in which the equilibrium configuration is the result of opposing interactions can substantially disturb the equilibrium (at least locally), and the configuration around the impurity center will change. Let us illustrate this with the case in which the JT ions form a simple cubic lattice (notice that the strongest interaction in the garnets corresponds to precisely such a lattice) in which one JT center has been replaced by an impurity ion. It is easy to show that, in the case when there is local reconstruction, the energy difference (ΔE) between the original and reconstructed configurations can be written in terms of the parameters J_{ee}^A and J_{gg}^A in accordance with the relations (8):

$$\Delta E = -\frac{3}{2}(J_{gg}^A + 3J_{ee}^A). \quad (\text{B})$$

On account of the inequalities (8), ΔE is negative, and, consequently, the reconstruction lowers the energy of the system. At the same time it drastically reduces the net deformation of the unit cell. To prove this, we need only compute the change in $\sum_i \cos \varphi_i$. Taking into account the fact that $\cos \varphi_i = 1$ in the case when the i -th octahedron is tetragonally distorted along the z axis and $\cos \varphi_i = -1/2$ when the tetragonal distortion is along the x or y axis, we can show that the considered reconstruction of the structure decreases the magnitude of the unit-cell distortion by a factor of seven.

Thus, it follows from the above-considered model that the substitution of even a small number of the JT ions leads to the "suppression" of the CJTE, which is the cause of the high critical JT-ion concentration values for the garnet structure.

4.2. Temperature dependence of the deformation

The temperature dependence of the order parameter (ξ) can be calculated from the energy (11) in the molecular-field approximation. To do this, we must, using the Boltzmann statistics, find for each of the four sublattices at fixed temperature T the mean values $\overline{\cos \varphi_i}$ and $\overline{\sin \varphi_i}$:

$$\overline{\cos \varphi_i} = \frac{1}{Z_i} \int_0^{2\pi} \cos \varphi_i \exp\left(\frac{-E_i}{kT}\right) d\varphi_i, \quad (13)$$

$$\overline{\sin \varphi_i} = \frac{1}{Z_i} \int_0^{2\pi} \sin \varphi_i \exp\left(\frac{-E_i}{kT}\right) d\varphi_i,$$

where

$$Z_i = \int_0^{2\pi} \exp(-E_i/kT) d\varphi_i, \quad (\text{C})$$

while the energy E_i is determined from the formula (11) by replacing $\cos \varphi_j$ and $\sin \varphi_j$ (for $j \neq i$) by their mean values. Solving (13) by the method of successive approximations (starting from a low temperature T_0 at which $\overline{\cos \varphi_i}$ and $\overline{\sin \varphi_i}$ are close to the equilibrium values at 0 K), we computed the free energies of the ordered and disordered states for each temperature. The temperature T_{JT} was then determined from the requirement that these two energies be equal. It turns out that, for both configurations (A_1 and A_2), T_{JT} does not depend on J_1 :

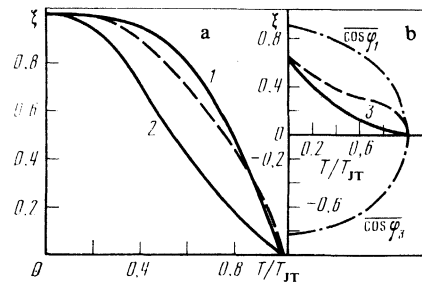


FIG. 12. Theoretical (continuous lines) and experimental (dashed lines) order-parameter—versus—reduced-temperature curves for: a) CuVG; b) MnGeG. The curve 1 corresponds to the computation with the parameters $J_0/K = 0.3$, $J_1/K = -0.2$, and $a = 0$; the curve 2, to the computation with $J_0/K = 0.6$, $J_1/K = -0.2$, and $a = 0$. The theoretical curves b) were calculated with the parameters $J_0/K = 7$, $J_1/K = 0.2$, and $a = 0$. The dot-dashed curve shows the contributions of the sublattices 1 and 3 to the order parameter (the scale for the total curve 3 along the ordinate axis has been increased by a factor of 10).

$$kT_{JT} = \frac{1}{2}(J_0 + a/2).$$

It should be noted that, since the energy (11) is invariant under the interchanges $1 \leftrightarrow 4$, $2 \leftrightarrow 3$, and $1, 4 \leftrightarrow 3, 2$ of the centers, the phase transition is of second order for all values of the parameters. The reason for this was first given by Kanamori in his analysis of the CJTE in the perovskites.⁷

In Fig. 12 we compare the theoretical and experimental order parameter (macroscopic strain)—versus— T/T_{JT} curves for the configurations A_1 (CuVG) and A_2 (MnGeG). Notice that, for A_1 [Fig. 12(a)], the contributions of the individual sublattices to ξ are equal ($\overline{\cos \varphi_i}$ does not depend on i here); therefore, the theoretical $\xi(T/T_{JT})$ curves also characterize the variation of $\overline{\cos \varphi_i}$ with temperature. For the configuration A_2 [Fig. 12(b)], we give the contributions of the individual sublattices, their sum, and the experimental results. It can be seen that in the case of CuVG the agreement of the theory with experiment is satisfactory, an assertion which cannot be made in the MnGeG case. It is possible that, since in the latter case the small net distortion is given by the difference between two large quantities, the molecular-field approximation used by us and the neglect of the interactions with more distant neighbors have a significant effect on the results of the calculation.

4.3. The magnetic properties

The results of the measurements of the magnetic and magnetostriction properties of MnGaGeG indicate that samples with long-range antiferromagnetic order undergo a metamagnetic transition in an external magnetic field at a temperature below T_N . In a MnGeG single crystal the values of the critical fields H_{cr} , i.e., the field-intensity values at which the magnetization and magnetostriction jumps occur, essentially depend on the direction of the field \mathbf{H} in the crystal. In this case, for all directions of \mathbf{H} , the magnetization value after the jump is equal to $\sim 25\%$ of the saturation magnetization at 0 K, i.e., a total flop of the sublattices does not occur in MnGeG, as in the case of a uniaxial two-sublattice antiferromagnet with anisotropy energy higher than the

exchange energy. Notice also that the extrapolation of the $M(H)$ curves for $H > H_{cr}$ to the value $H = 0$ yields a nonzero M value.

The indicated characteristics of the magnetic behavior of the MnGeG crystal can, in our opinion, be qualitatively explained within the framework of a model in which the crystal is considered to be multisublattice noncollinear metamagnet anisotropy energy is comparable to the exchange energy. Kugel and Khomskii²⁴ conjecture that the phase transition that occurs in MnGeG in a magnetic field below T_N is connected with a change in the ordering of the orbitals. According to our measurements, at 4.2 K the jump in the magnetostriction along the [001] axis (H was parallel to the direction in which the distortion was measured) is 15×10^{-6} , and does not exceed the value 5×10^{-6} in the other directions.

Thus, if the magnetic transition in MnGeG does have effect on the orbital ordering, the effect is quite insignificant. The transition from the configuration A_2 to A_1 , for example, should, in our opinion, be accompanied by a magnetostriction of the order of the magnitude of the crystal-lattice distortion, i.e., $\sim 10^{-3}$. Consequently, it can be assumed that the magnetic phase transition that occurs in MnGeG below T_N is due to a change in the antiferromagnetic structure of this garnet in the external magnetic field.

A different situation is observed for the investigated MnGaGeG samples, in which the distortions induced by the JT centers have an uncorrelated character. Figure 13 shows the x dependence of $\Delta l/l$ at 4.2 K for paramagnetic manganese garnets ($x \leq 1.0$). It can be seen that the variation of the magnetostriction (in a field of intensity $H = 40$ kOe) with concentration exhibits at $x = 0.5$ a peak unrelated to the dependence $\chi(x)$. The $\chi(x)$ peak, which is due to the appearance of short-range magnetic order, corresponds to $x = 1.0$. Consequently, it can be assumed that the observed x dependence of the magnetostriction $\Delta l/l$ of paramagnetic MnGaGeG is due to the contribution to the "normal" magnetostriction of the effects of the orientation by the external magnetic field of the axes of the local distortions of the JT clusters. According to Dionne,²⁵ ions with an orbitally degenerate ground state induce local distortions whose axes are uniformly distributed over all the equivalent axes of the cubic crystal. One of the axes becomes preferred when the crystal is placed in an external magnetic field, and a reorientation of the distortions

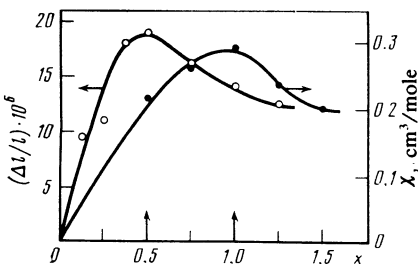


FIG. 13. Dependence of the magnetostriction $\Delta l/l$ and the magnetic susceptibility χ on the Mn^{3+} -ion concentration in MnGaGeG at 4.2 K in a field of intensity $H = 40$ kOe.

toward this axis occurs which leads to an additional contribution to the magnetostriction.

4.4. The Jahn-Teller effect in garnets with concentrations lower than the critical concentration

The experimental data presented in Subsec. 2.3 indicate the growth in the region $T < 40$ K of acoustic losses in the garnets in which the CJTE does not occur (Figs. 4 and 5). Gyorgy *et al.* report in Ref. 26 the effect of small concentrations ($\sim 0.01\%$) of the JT ions Ni^{3+} and Mn^{2+} on the acoustic properties of $Y_3Al_5O_{12}$ and Al_2O_3 single crystals. Below 20 K they observed an increase in the acoustic losses, which was accompanied by a decrease in the elastic constants ($\delta E \approx 0.1\%$). These effects are due to relaxational processes involving mechanical-stress-induced transitions between the various directions of the JT distortions.

On the other hand, in the garnets investigated by us, a decrease in the temperature leads to an increase in E , which increase clearly indicates a decrease in the probability for passage through the potential barrier at the expense of the thermal-excitation energy, i.e., indicates the conversion of the dynamical JTE into the static effect. The thermal-excitation energy at $T \approx 30$ K is of the order of the height of the barriers between the minima of the potential energy of the E term of the JT complex, and a "freezing" of the directions of the local distortions occurs which is accompanied by an increase in the rigidity of the lattice, i.e., by an increase in E . The nonmonotonic dependence of the low-temperature anomaly on the concentration of the JT ions is apparently due to the fact that the effective contribution to this anomaly is made not by all the JT ions, but by only cluster-forming small groups of them. As impurity ions are introduced into the sample, the number of such clusters at first increases (the "pulverization" of the clusters), and then begins to decrease. Let us note that, as can be seen from Fig. 4, the garnets in which the CJTE occurs (in particular, MnGeG) also exhibit some increase in E at low temperatures. This allows us to postulate the existence in MnGeG of a small number of "uncorrelated" Mn^{3+} ions even in the absence of impurity centers, which is, in principle, permitted by the crystal chemistry of compounds with the garnet structure.

5. CONCLUSION

The experimental investigations and the theoretical analysis carried out in the present work characterize certain mechanisms underlying the appearance of the CJTE in materials with the garnet structure. The results of the work show that octahedral Mn^{3+} and Cu^{2+} ions with the E_g electronic ground state give rise to a number of anomalies in the garnets: unusual relations between T_{JT} and the magnitudes of the tetragonal distortions, high critical JT-ion concentration values, unusual temperature dependences of the order parameter, unique magnetic and elastic properties in the region of liquid-helium temperatures, etc.

We have been able to qualitatively describe on the basis of a relatively simple model the set of experimental data on the CJTE in the garnets with the aid of four parameters — K , a , J_0 , and J_1 . A quantitative analysis requires the theo-

retical calculation, or an independent determination, of these parameters. For the relative magnitudes of J_0 , J_1 , and a , this can be done either on the basis of the theory of elasticity, or with the use of the methods employed in lattice-dynamics investigations. The case of the anisotropy parameter K , for which, in our opinion, there is at present no reliable computational method, is more complicated. But we can obtain a rough estimate that characterizes the ratio of K to the pair-interaction constants. For this purpose, it is sufficient to compare the magnitudes of the tetragonal distortions in the ferroelastically-ordered spinels Mn_3O_4 (15×10^{-2}) and $CuFe_2O_4$ (6×10^{-2}) (Ref. 20) with the corresponding values for MnGeG and CuVG (we neglect the deviation of the linear vibronic coupling constant and the elastic constants of the garnets from the corresponding constants of the spinels). As follows from Fig. 11, the large magnitude of the distortion in the spinels corresponds to a small value for the ratio of the pair-interaction constants to the anisotropy, and can be used as the scale along the ordinate axis in Fig. 11. Then, allowing for the fact that the axes of the octahedrons in the garnets are not parallel to each other, and using Fig. 11, we find that $|J_0 + a/2|/K \sim 4-7$ for MnGeG and $|J_0 + J_1 + a/2|/K < 0.5$ for CuVG. From this we draw the conclusion that the anisotropy in a garnet with Cu^{2+} is high, while the pair interactions predominate in a manganese garnet.

In the present paper we not discuss the dynamical aspects of the JTE in the garnets. Let us note, however, that our method of computing the temperature dependence of the distortion (Subsec. 4.2) is the classical analog of the method used by Englman and Halperin^{5,6} to analyze the temperature dependence of the CJTE in the spinels and the perovskites. Here the dynamical effects (in the scheme of the Englman-Halperin approach) can be taken into account if, instead of the classical energy (11), we proceed from the corresponding Hamiltonian, and compute the free energy with the aid of its eigenvalues. The indicated circumstance does not, in our opinion, specify the rigor of the proposed treatment, which contains cruder approximations, e.g., the neglect of the interactions with more distant neighbors.

Let us also note that we virtually did not discuss the interrelationship between the CJTE and the magnetic properties of the garnets. This question is, in our opinion, of indubitable interest, and requires further experimental and theoretical investigations.

The authors are grateful to K. P. Belov and S. Krupicka for constant interest in the work and to B. V. Mill' for growing the MnGeG single crystals and helping in the preparation of the polycrystalline samples.

APPENDIX

Here we give a brief qualitative analysis of the effect on the JTE of the trigonal distortion and the nonparallelism of the axes of the octahedrons in the garnets. To begin with, let us note that, even for an isolated JT center, allowance for the trigonal distortion leads to the existence of two pairs of E_g normal coordinates, with which the electronic doublet can interact linearly. This difficulty can, according to Ref. 27, be

overcome by taking into account the fact that the interaction is strong only for that pair of E_g coordinates which goes over in the limit of zero trigonal distortion into Q_ϕ , Q_e .

Furthermore, the indicated characteristic of the garnet structure should be taken into consideration in an analysis of the pair interactions between the JT centers. For the configurations A and B , the equalities (9) will not be satisfied, i.e.,

$$J_{e\phi}^A, J_{\phi z}^A, J_{e\phi}^B, J_{\phi z}^B \neq 0; \quad J_{ee}^B \neq J_{\phi\phi}^B.$$

But since each octahedral site continues to have the symmetry C_3 , we can easily show that equalities similar to (9) will be satisfied, not for the individual pairs, but for the total interactions. Indeed, if the center i belongs to, say, the sublattice 1 and the centers j are its nearest neighbors from any of the sublattices 2, 3, and 4, then the C_3 symmetry leads to the relations

$$\sum_j J_{ee}^{ij} = \sum_j J_{\phi\phi}^{ij}, \quad \sum_j J_{e\phi}^{ij} = - \sum_j J_{\phi e}^{ij}.$$

These equalities do not change the form of the energy (11) even when the trigonal distortions are taken into consideration, and, consequently, all the results concerning the stability of substituted JT systems and the temperature dependences also remain unchanged. It should, however, be noted that if the division into sublattices will be different and the C_3 symmetry will be broken, then a number of new independent parameters will appear in the formula for the energy.

¹Member of staff on the Institute of Physics, Academy of Sciences of the Czechoslovakian SSR, Prague.

²We detected antiferromagnetic order in the copper garnet at $T = 0.2$ K when the paper was ready for the press.

¹M. D. Sturge, *Solid State Phys.* **20**, 91 (1967).

²R. Englman, *The Jahn-Teller Effect in Molecules and Crystals*, Wiley-Interscience, New York, 1972.

³G. A. Gehring and K. A. Gehring, *Rep. Prog. Phys.* **38**, 189 (1975).

⁴K. I. Kugel' and D. I. Khomskii, *Usp. Fiz. Nauk* **136**, 621 (1982) [*Sov. Phys. Usp.* **25**, 231 (1982)].

⁵R. Englman and B. Halperin, *Phys. Rev. B* **2**, 75 (1970).

⁶B. Halperin and R. Englman, *Phys. Rev. B* **3**, 1698 (1971).

⁷Z. A. Kazei, B. V. Mill', and V. I. Sokolov, *Pis'ma Zh. Eksp. Teor. Fiz.* **24**, 229 (1976) [*JETP Lett.* **24**, 203 (1976)].

⁸P. Novák, *J. Phys. C* **14**, L293 (1981).

⁹K. P. Belov, B. V. Mill', G. Ronniger, V. I. Sokolov, and T. D. Hyen *Fiz. Tverd. Tela (Leningrad)* **12**, 1761 (1970) [*Sov. Phys. Solid State* **12**, 1393 (1970)].

¹⁰K. P. Belov, T. V. Valyanskaya, L. G. Mamsurova, and V. I. Sokolov, *Zh. Eksp. Teor. Fiz.* **65**, 1133 (1973) [*Sov. Phys. JETP* **38**, 561 (1974)].

¹¹R. Plumier and M. Sougi, *J. Phys. Lett.* **40**, 213 (1979).

¹²R. Plumier and D. Estève, *Solid State Commun.* **31**, 921 (1979).

¹³Z. A. Kazei, B. V. Mill', and V. I. Sokolov, *Pis'ma Zh. Eksp. Teor. Fiz.* **31**, 338 (1980) [*JETP Lett.* **31**, 308 (1980)].

¹⁴D. Estève, R. Plumier, P. Feldman, and H. Le Gall, *Phys. Status Solidi A* **57**, K83 (1980).

¹⁵V. I. Sokolov, *Prib. Tekh. Eksp. No. 5*, 206 (1975).

¹⁶Z. A. Kazei, M. V. Levanidov, and V. I. Sokolov, *Prib. Tekh. Eksp. No. 1*, 196 (1982).

¹⁷K. P. Belov, B. V. Mill', and V. I. Sokolov, in: *Fizika i khimiya ferritov (The Physics and Chemistry of the Ferrites)*, MGU, Moscow, 1973, p. 25.

¹⁸F. School and K. Binder, *Z. Phys. B* **39**, 239 (1980).

¹⁹E. Fawcett and G. K. White, *J. Appl. Phys.* **39**, 576 (1968).

²⁰J. B. Goodenough, *Magnetism and the Chemical Bond*, Interscience, New York, 1963 (Russ. Transl., Metallurgiya, Moscow, 1968).

- ²¹P. Novák, *J. Phys. Chem. Solids* **30**, 2537 (1969).
²²P. Holba, M. Nevřiva, and E. Pollert, *Mater. Res. Bull.* **10**, 853 (1975).
²³J. Kanamori, *J. Appl. Phys.* **31**, 149 (1960).
²⁴K. I. Kugel' and D. I. Khomskii, *Pis'ma Zh. Eksp. Teor. Fiz.* **23**, 264 (1976) [*JETP Lett.* **23**, 237 (1976)].
²⁵G. F. Dionne, *J. Appl. Phys.* **50**, 4263 (1979).
- ²⁶E. M. Gyorgy, R. C. LeGraw, and M. D. Sturge, *J. Appl. Phys.* **37**, 1303 (1966).
²⁷C. A. Bates and J. M. Dixon, *J. Phys. C* **2**, 2209 (1969).

Translated by A. K. Agyei